THE JOURNAL OF PHYSICAL CHEMISTRY LETTERS
A JOURNAL OF THE AMERICAN CHEMICAL SOCIETY

pubs.acs.org/JPCL

Letter

Suppression of X-ray-Induced Radiation Damage to Biomolecules in Aqueous Environments by Immediate Intermolecular Decay of Inner-Shell Vacancies

Andreas Hans,* Philipp Schmidt, Catmarna Küstner-Wetekam, Florian Trinter, Sascha Deinert, Dana Bloß, Johannes H. Viehmann, Rebecca Schaf, Miriam Gerstel, Clara M. Saak, Jens Buck, Stephan Klumpp, Gregor Hartmann, Lorenz S. Cederbaum, Nikolai V. Kryzhevoi,* and André Knie

Cite This: *J. Phys. Chem. Lett.* 2021, 12, 7146–7150

Read Online

ACCESS | Metrics & More | Article Recommendations | Supporting Information

ABSTRACT: The predominant reason for the damaging power of high-energy radiation is multiple ionization of a molecule, either direct or via the decay of highly excited intermediates, as, e.g., in the case of X-ray irradiation. Consequently, the molecule is irreparably damaged by the subsequent fragmentation in a Coulomb explosion. In an aqueous environment, however, it has been observed that irradiated molecules may be saved from fragmentation presumably by charge and energy dissipation mechanisms. Here, we show that the protective effect of the environment sets in even earlier than hitherto expected, namely immediately after single inner-shell ionization. By combining coincidence measurements of the fragmentation of X-ray-irradiated microsolvated pyrimidine molecules with theoretical calculations, we identify direct intermolecular electronic decay as the protective mechanism, outrunning the usually dominant Auger decay. Our results demonstrate that such processes play a key role in charge delocalization and have to be considered in investigations and models on high-energy radiation damage in realistic environments.

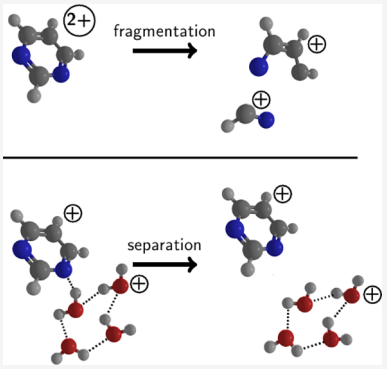

The exposure to ionizing radiation is known to have severe consequences to living organisms. Depending on the radiation dose, the organism may suffer from cytotoxic effects ranging from enhanced cancer risk to radiation sickness. Notwithstanding the macroscopic symptoms, the radiation damage itself happens on a molecular level.[1]

As a common assumption, about two-thirds of such damage is an *indirect* and purely environmental effect caused by secondary low-energy electrons and radicals[1−4] originating in radiolysis of water monomers surrounding biomolecules. The rest results from *direct* deposition of energy in biomolecules. It is tempting to assume that the indirect damage owes its predominance to simply the large amount of water in biological tissue. The situation is, however, more complicated, and recent works suggest that the contribution from direct and indirect processes is still not well understood.[3,5]

As evidenced by recent ion-impact experiments on several hydrated biomolecules,[6−10] an aqueous environment is able to significantly suppress the direct damage and thus play an "unusual" role of a damage protector. This striking protective effect was ascribed to the environmental ability to absorb and dissipate the energy transferred to biomolecules in collisions.[7,11] If the radiation damage was induced by multiple ionization, charge redistribution from localized states to delocalized ones was also considered among the potential protection mechanisms. In the present study, we demonstrate that the water environment starts to protect biomolecules exposed to radiation even before ultrafast autoionization converts these molecules into highly unstable multiply charged systems.

In case of X-ray element-specific irradiation, the radiobiologically most relevant process is inner-shell ionization of one of the constituting atoms of a biomolecule, forming highly excited states with vacancies in a core orbital. Such highly excited species relax predominantly via Auger decay, in which one electron of the molecular valence orbitals fills the core vacancy and another valence electron is released, resulting in dissociative multiply charged states. The consequences, namely inevitable destruction by fragmentation, are well investigated for isolated molecules.[12−20]

We investigated the X-ray-induced fragmentation of microsolvated pyrimidine in a photoelectron-photoion-photoion coincidence (PEPIPICO) experiment (see Experimental Methods). Being one of the building blocks of nucleobases and therefore of larger biomolecules, pyrimidine ($C_4H_4N_2$)

Received: June 13, 2021
Accepted: July 20, 2021
Published: July 23, 2021

serves as a prototype system for many fundamental investigations.[15,20] Its photochemistry is especially relevant for various medical applications, in which halogenated pyrimidines are used as radiosensitizers.[21] The core ionization of isolated pyrimidine and its derivatives is known to cause the fragmentation of the molecule into two or more ionic fragments.[14,15] Thus, no parent ions or doubly charged molecular fragments are observed in coincidence with core electrons, which is in agreement with the present work.

In contrast, for microsolvated pyrimidine, we observe intact parent ions in coincidence with water cluster ions and carbon photoelectrons. The corresponding ion−ion coincidence map is shown in Figure 1a. The mass-to-charge ratio of the pyrimidine

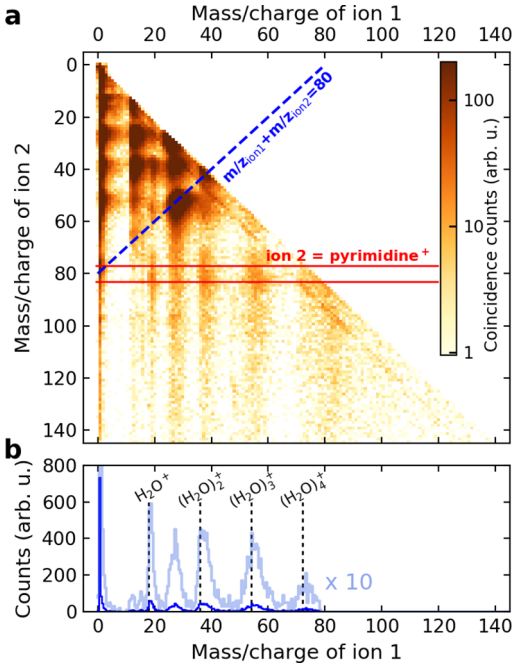

Figure 1. Photoelectron−photoion−photoion coincidence spectra from a target jet containing both isolated and microsolvated pyrimidine molecules, ionized with soft X-rays of 300 eV photon energy. (a) Ion−ion map for coincidences of a carbon core photoelectron and two ions. (b) Spectrum of ion 1, selected for ion 2 being the pyrimidine parent ion (dark blue trace) and 10-fold magnified (light blue trace).

parent ion is m/z = 80. Prominent features appear in the coincidence map on the m/z = 80 diagonal or to the upper left of it, i.e., for pairs of singly charged ions whose sum of masses is 80 atomic units or less. These features mainly originate from ionization of isolated pyrimidine molecules, which occur abundantly in the target (see Experimental Methods).

Importantly, however, a significant signal is observed for ion pairs with one of the ions having the mass of the pyrimidine parent ion, i.e., 80 atomic units, emphasized between the red lines in Figure 1a. To obtain insight into the underlying fragmentation processes, the spectrum of the ions observed *in coincidence* with said parent ion is shown in Figure 1b.

The most prominent feature in this spectrum is a series of water cluster ions at integer multiple masses of the water molecule (m/z_{H2O} = 18). The slight shift of the peak centers to higher masses compared to the theoretical water cluster ion masses (displayed by dashed vertical bars) may indicate protonation of the water cluster ions, a common observation in the fragmentation of water clusters.[22] Additionally, two peaks are observed at m/z = 1 and m/z = 26−28, which can be attributed to single protons and the pyrimidine fragments $C_2H_2^+$ and CH_2N^+. Their appearance is explained by clusters containing more than one pyrimidine molecule, allowing fragmentation into pyrimidine parent ions and molecular fragments.

In order to identify the mechanisms responsible for the experimental observations, we performed calculations on the decay of core vacancies in microsolvated pyrimidine molecules (see Supporting Information for computational details). The electron spectra resulting from the decay of carbon core vacancies of isolated and tetrasolvated pyrimidine are shown in Figure 2, parts a and b. The spectra are averaged over all carbon atoms of the molecule. The Auger spectrum of isolated pyrimidine (panel a) agrees well with earlier experimental and theoretical reports.[23] The total electron spectrum of 4-fold hydrated pyrimidine (red trace in panel b) is overall very similarly shaped compared to that of isolated pyrimidine. However, a closer look shows a dramatic difference in the nature

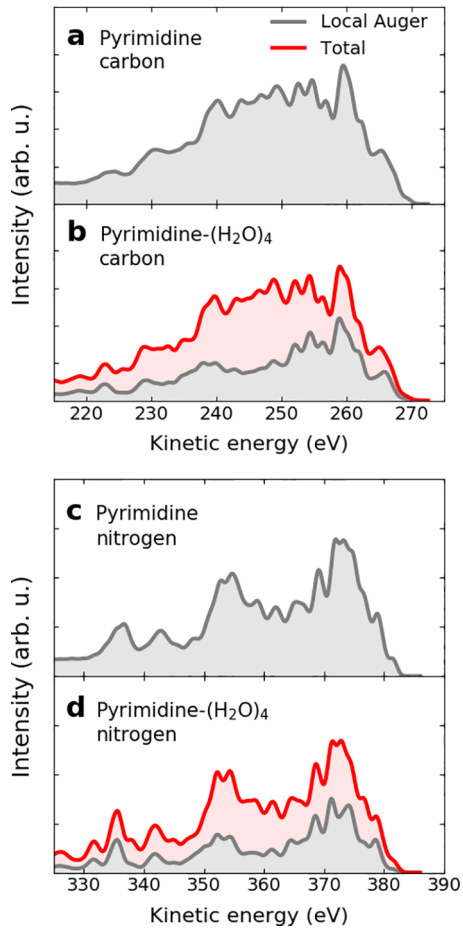

Figure 2. Calculated electron spectra resulting from the decay of core vacancies in pyrimidine molecules. (a) Auger spectrum of isolated pyrimidine after carbon core ionization, averaged over all carbon atoms. (b) Total spectrum of pyrimidine solvated by four water molecules (red) and the contribution of local Auger decay (gray) after carbon core ionization. (c) Auger spectrum of isolated pyrimidine after nitrogen core ionization, averaged over both nitrogen atoms. (d) Total spectrum of pyrimidine solvated by four water molecules (red) and the contribution of local Auger decay (gray) after nitrogen core ionization. In panels b and d, the red shaded area corresponds to nonlocal intermolecular channels.

https://doi.org/10.1021/acs.jpclett.1c01879
J. Phys. Chem. Lett. 2021, 12, 7146−7150

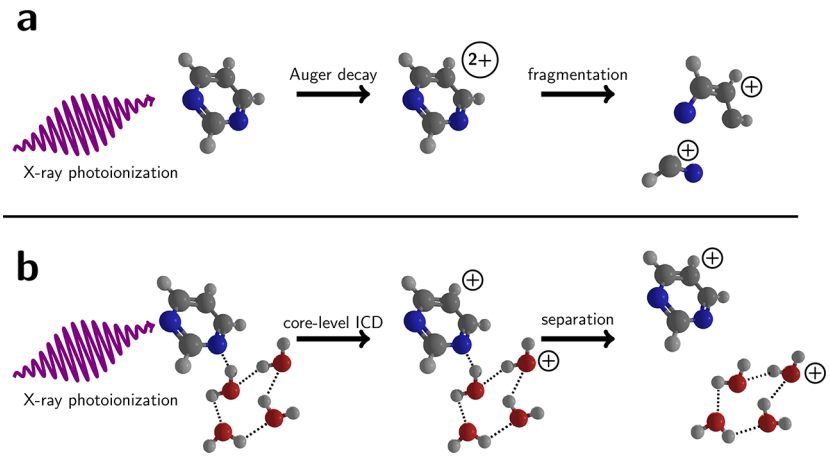

Figure 3. Schematic of the observed process. (a) X-ray photoionization of a biomolecule is followed by Auger decay into doubly charged molecular states. As a consequence, the molecule dissociates into ionic fragments. (b) If the molecule is solvated, intermolecular decay processes like core-level ICD become operable, which distribute charge to the environment and thereby protect the molecule from fragmentation.

of the final states. Only a minor part (gray trace in panel b) of the spectrum corresponds to dicationic states for which both charges are localized at the pyrimidine molecule. The difference between the total spectrum (red trace) and the localized dicationic contribution corresponds to delocalized final states, for which the second electron was emitted from the environment, having direct implications on the subsequent fragmentation of the system. A very similar behavior is observed for core ionization of nitrogen atoms, and the corresponding spectra are shown in Figure 2, parts c and d. Exploration of the configurations of the final states reveals core-level intermolecular Coulombic decay[24−26] (core ICD) as the dominant nonlocal decay (see the Supporting Information for a precise description of the contributing channels). In this mechanism, a core vacancy is filled by a valence electron of the pyrimidine, and a valence electron from a neighboring water molecule is emitted. ICD and related processes were recently predicted and observed to significantly contribute to the secondary electron spectra of core and inner-valence vacancies in dense media.[27−32] A second contributing process is core-level electron-transfer-mediated-decay (core ETMD), which may occur in two variants. In ETMD(2), the core vacancy is filled by a valence electron of a neighboring water molecule, and another valence electron of the same molecule is ejected. ETMD(3) involves three molecules, and the released electron originates from yet another adjacent water molecule.

Remarkably, while ICD and ETMD usually dominate only if local electron emission is energetically forbidden, in the present case, they outrun even Auger decay, which is typically the dominant decay route of core vacancies. As one possible consequence of ICD, the pyrimidine molecule and the hydration shell separate by Coulomb repulsion and are observable as pyrimidine parent ion and water cluster ion, matching well with the experimental observation.

For a pyrimidine molecule solvated by only four water molecules, our calculations predict a remarkable ratio of 58% of carbon core vacancies decaying by intermolecular processes. This value grows from 0% to 24%, 41%, and 50% for solvation by 0, 1, 2, and 3 water molecules, respectively (see Supporting Information for ionization of nitrogen) and is expected to be even larger for fully solvated molecules.

From the present experimental spectra, the ratio of local to intermolecular decay cannot be deduced, since the exact composition of the target gas jet (isolated pyrimidine, water, pyrimidine molecules hydrated by different numbers of water molecules) is not known accurately. For similar reasons, the exact fraction of molecules, which are protected from fragmentation by the intermolecular decay, is unknown. While some of the final states may still be dissociative (producing pyrimidine fragment ions and neutral fragments), the stable parent ion is known to dominate the mass spectrum after valence ionization.[20,33] We envision further final state selective studies to quantify the extent of the protection. The protection effect of the solvation against X-ray-induced radiation damage is illustrated in Figure 3, which schematically shows how different the fates of isolated pyrimidine (panel a) and solvated (panel b) pyrimidine are upon inner-shell ionization.

The relevance of ICD for radiobiology has been discussed intensely throughout the years after its prediction in 1997.[34−37] Within this discussion, mainly the role of emerging secondary electrons, ions, and radicals contributing to the indirect radiation damage is considered. These particles with damaging potential are the products of ICD of inner-valence vacancies[29,34] or in the case where ICD is part of a decay cascade and occurs subsequently to local Auger decay.[35,36] In the present work, we reveal the importance of the core-level variant of ICD as damage protector by demonstrating its decisive role for the fate of a core-ionized biomolecule reducing the direct damage substantially. Our findings imply that models on radiation damage need to be revisited if the damage is mediated by dissociation of multiply charged molecular states, which are populated via excited intermediates. First, the aqueous environment of a biorelevant molecule starts to intervene early and may drastically change the decay route of excited intermediates before reaching the dissociative state. Second, the products of individual photon−molecule interactions, such as electrons, ions, and radicals, differ qualitatively. Since these products and their properties are considered as the starting conditions for indirect radiation damage, the referring models are also directly affected.

For proper assessment of the radiobiological effect of X-rays, knowledge about the radiation chemistry of ionized solvated molecules is required. X-ray-based radiotherapy mainly relies on the direct damaging effect to biomolecules. Ion radiotherapy turned out to be significantly advantageous compared to X-ray radiotherapy in many points, with the main reason being the lateral concentration of radiation dose.[38] It is another interesting

https://doi.org/10.1021/acs.jpclett.1c01879
J. Phys. Chem. Lett. 2021, 12, 7146−7150

aspect that destructive multiply charged molecular states are typically directly induced by ion impact, while they are populated via excited intermediates after X-ray ionization. Intermolecular decay processes as observed here may thus contribute to the lower efficiency of X-ray radiation therapies.

EXPERIMENTAL METHODS

The experiment was performed at the P04 beamline of the PETRA III synchrotron radiation facility in Hamburg.[39] The storage ring was operated in 40-bunch mode, delivering light pulses to the beamline with about 192 ns temporal spacing. A photoelectron−photoion−coincidence (PEPICO) setup available at the beamline was used. The working principle is similar to the one described in ref 40. The electron spectrometer is a magnetic bottle type time-of-flight spectrometer, and the drift tube is equipped with several retardation stages. The permanent magnet, which is used in this type of spectrometers to guide the electrons into the electron drift tube, is ring-shaped and simultaneously is part of the 23 mm long ion drift tube of the ion time-of-flight spectrometer. The ion extraction potential is applied continuously. Therefore, a continuous stable operation without voltage pulsing is possible, however, with the drawback of a limited resolution in both electron and ion spectra. From our ion time-of-flight spectra we estimated a resolution of $(m/z)/\Delta(m/z) \approx 15$. In the electron spectra, photoelectrons and Auger electrons, which are by far the dominant contribution at the used photon energies, are well separated. No further differentiation was attempted. Both ion and electron spectrometer are equipped with a chevron microchannel plate stack to detect electron and ion emission.

Microhydrated pyrimidine molecules were produced by supersonic coexpansion of the vapor of a mixture of liquid water and pyrimidine (94% water, 6% pyrimidine) through a conical copper nozzle (80 μm diameter, 30° opening angle) into vacuum. To increase the vapor pressure, the liquid mixture was heated to 80 °C. The formation of hydrated molecules under these conditions was confirmed prior to the beamtime in preparatory experiments using a commercial quadrupole mass spectrometer. The ratio of microhydrated molecules is typically in the order of a few percent of the overall target jet. Beside the production of single pyrimidine molecules embedded in a water cluster, the formation of clusters with several pyrimidine molecules is possible but expected to be weak. Note that using this procedure of sample preparation, the appearance of isolated, gaseous water and pyrimidine molecules cannot be avoided. See the Supporting Information for a representative mass spectrum obtained with similar conditions.

The expansion chamber was separated from the interaction chamber by a skimmer with 0.7 mm orifice diameter. The typical pressure inside the interaction chamber during operation was about 3×10^{-6} mbar.

ASSOCIATED CONTENT

Supporting Information

The Supporting Information is available free of charge at https://pubs.acs.org/doi/10.1021/acs.jpclett.1c01879.

Detailed description of the data acquisition and analysis procedure, computational details, exemplary target mass spectrum, individual channels contributing to the decay of core vacancies in C and N atoms in microsolvated pyrimidine, and calculated integrated contribution of local Auger decay to the total decay (PDF)

AUTHOR INFORMATION

Corresponding Authors

Andreas Hans − *Institut für Physik und CINSaT, Universität Kassel, 34132 Kassel, Germany;* orcid.org/0000-0002-4176-4766; Email: hans@physik.uni-kassel.de

Nikolai V. Kryzhevoi − *Theoretische Chemie, Physikalisch-Chemisches Institut, Universität Heidelberg, 69120 Heidelberg, Germany*; Email: nikolai.kryzhevoi@pci.uni-heidelberg.de

Authors

Philipp Schmidt − *Institut für Physik und CINSaT, Universität Kassel, 34132 Kassel, Germany; European XFEL, 22869 Schenefeld, Germany*

Catmarna Küstner-Wetekam − *Institut für Physik und CINSaT, Universität Kassel, 34132 Kassel, Germany*

Florian Trinter − *Deutsches Elektronen-Synchrotron (DESY), 22607 Hamburg, Germany; Molecular Physics, Fritz-Haber-Institut der Max-Planck-Gesellschaft, 14195 Berlin, Germany;* orcid.org/0000-0002-0891-9180

Sascha Deinert − *Deutsches Elektronen-Synchrotron (DESY), 22607 Hamburg, Germany*

Dana Bloß − *Institut für Physik und CINSaT, Universität Kassel, 34132 Kassel, Germany*

Johannes H. Viehmann − *Institut für Physik und CINSaT, Universität Kassel, 34132 Kassel, Germany*

Rebecca Schaf − *Institut für Physik und CINSaT, Universität Kassel, 34132 Kassel, Germany*

Miriam Gerstel − *Institut für Physik und CINSaT, Universität Kassel, 34132 Kassel, Germany*

Clara M. Saak − *Molecular and Condensed Matter Physics Division, Department of Physics and Astronomy, Uppsala University, 75120 Uppsala, Sweden;* orcid.org/0000-0001-7898-0713

Jens Buck − *Deutsches Elektronen-Synchrotron (DESY), 22607 Hamburg, Germany*

Stephan Klumpp − *Deutsches Elektronen-Synchrotron (DESY), 22607 Hamburg, Germany*

Gregor Hartmann − *Institut für Physik und CINSaT, Universität Kassel, 34132 Kassel, Germany; Helmholtz-Zentrum Berlin (HZB), 12489 Berlin, Germany*

Lorenz S. Cederbaum − *Theoretische Chemie, Physikalisch-Chemisches Institut, Universität Heidelberg, 69120 Heidelberg, Germany;* orcid.org/0000-0002-4598-0650

André Knie − *Institut für Physik und CINSaT, Universität Kassel, 34132 Kassel, Germany;* orcid.org/0000-0002-2208-8838

Complete contact information is available at: https://pubs.acs.org/10.1021/acs.jpclett.1c01879

Notes

The authors declare no competing financial interest.

ACKNOWLEDGMENTS

We acknowledge DESY (Hamburg, Germany), a member of the Helmholtz Association HGF, for the provision of experimental facilities. Parts of this research were carried out at PETRA III, and we would like to thank the P04 team for assistance in using the P04 beamline and the photoelectron−photoion coincidence spectrometer. This work was supported by the Deutsche Forschungsgemeinschaft (via Research Unit FOR 1789 and Project No. 328961117−SFB 1319 ELCH). L.S.C. is grateful to

the European Research Council (Advanced Investigator Grant No. 692657) for financial support. F.T. acknowledges support by the MaxWater initiative of the Max-Planck-Gesellschaft. We also acknowledges the scientific exchange and support of the Center for Molecular Water Science.

REFERENCES

(1) *Radiation Damage in Biomolecular Systems*; García Gómez-Tejedor, G., Fuss, M. C., Eds.; Springer: Dordrecht, Heidelberg, London, and New York, 2012.
(2) Sanche, L. Beyond Radical Thinking. *Nature* **2009**, *461*, 358−359.
(3) Alizadeh, E.; Orlando, T. M.; Sanche, L. Biomolecular Damage Induced by Ionizing Radiation: The Direct and Indirect Effects of Low-Energy Electrons on DNA. *Annu. Rev. Phys. Chem.* **2015**, *66*, 379−398.
(4) Boudaïffa, B.; Cloutier, P.; Hunting, D.; Huels, M. A.; Sanche, L. Resonant Formation of DNA Strand Breaks by Low-Energy (3 to 20 eV) Electrons. *Science* **2000**, *287*, 1658−1660.
(5) Nguyen, J.; et al. Direct Observation of Ultrafast-Electron-Transfer Reactions Unravels High Effectiveness of Reductive DNA Damage. *Proc. Natl. Acad. Sci. U. S. A.* **2011**, *108*, 11778−11783.
(6) Maclot, S.; et al. Ion-Induced Fragmentation of Amino Acids: Effect of the Environment. *ChemPhysChem* **2011**, *12*, 930−936.
(7) López-Tarifa, P.; et al. Ultrafast Damage Following Radiation-Induced Oxidation of Uracil in Aqueous Solution. *Angew. Chem., Int. Ed.* **2013**, *52*, 3160−3163.
(8) Markush, P.; et al. The Role of the Environment in the Ion Induced Fragmentation of Uracil. *Phys. Chem. Chem. Phys.* **2016**, *18*, 16721−16729.
(9) Castrovilli, M. C.; et al. Fragmentation of Pure and Hydrated Clusters of 5Br-Uracil by Low Energy Carbon Ions: Observation of Hydrated Fragments. *Phys. Chem. Chem. Phys.* **2017**, *19*, 19807−19814.
(10) Nomura, S.; et al. Dissociation of Biomolecules in Liquid Environments During Fast Heavy-Ion Irradiation. *J. Chem. Phys.* **2017**, *147*, 225103.
(11) Gaigeot, M.-P.; et al. Theoretical Investigation of the Ultrafast Dissociation of Ionised Biomolecules Immersed in Water: Direct and Indirect Effects. *Mutat. Res., Rev. Mutat. Res.* **2010**, *704*, 45−53.
(12) Itälä, E.; et al. Fragmentation Patterns of Core-Ionized Thymine and 5-Bromouracil. *J. Chem. Phys.* **2010**, *133*, 154316.
(13) Itälä, E.; et al. Fragmentation Patterns of Core Ionized Uracil. *Int. J. Mass Spectrom.* **2011**, *306*, 82−90.
(14) Itälä, E.; et al. Molecular Fragmentation of Pyrimidine Derivatives Following Site-Selective Carbon Core Ionization. *J. Electron Spectrosc. Relat. Phenom.* **2011**, *184*, 119−124.
(15) Lin, Y.-S.; et al. Measurement and Prediction of the NEXAFS Spectra of Pyrimidine and Purine and the Dissociation Following the Core Excitation. *Chem. Phys. Lett.* **2015**, *636*, 146−153.
(16) Chiang, Y.-J.; Lin, Y.-S.; Lin, H.-R.; Liu, C.-L. Specific Dissociation of Core-Excited Pyrimidine Nucleobases. *Chem. Phys. Lett.* **2018**, *706*, 215−222.
(17) Inhester, L.; et al. Chemical Understanding of the Limited Site-Specificity in Molecular Inner-Shell Photofragmentation. *J. Phys. Chem. Lett.* **2018**, *9*, 1156−1163.
(18) López-Tarifa, P.; et al. Ultrafast Nonadiabatic Fragmentation Dynamics of Doubly Charged Uracil in a Gas Phase. *Phys. Rev. Lett.* **2011**, *107*, 023202.
(19) de Vries, J.; Hoekstra, R.; Morgenstern, R.; Schlathölter, T. Charge Driven Fragmentation of Nucleobases. *Phys. Rev. Lett.* **2003**, *91*, 053401.
(20) Bolognesi, P.; et al. Photofragmentation of Organic Molecules of Biological Interest: The Pyrimidine and 2Br-Pyrimidine Cases. *Nucl. Instrum. Methods Phys. Res., Sect. B* **2012**, *279*, 118−123.
(21) Mitchell, J. B.; Russo, A.; Cook, J. A.; Straus, K. L.; Glatstein, E. Radiobiology and Clinical Application of Halogenated Pyrimidine Radiosensitizers. *Int. J. Radiat. Biol.* **1989**, *56*, 827−836.
(22) Shiromaru, H.; Shinohara, H.; Washida, N.; Yoo, H.-S.; Kimura, K. Synchrotron Radiation Measurements of Appearance Potentials for $(H_2O)_2^+$, $(H_2O)_3^+$, $(H_2O)_2H^+$ and $(H_2O)_3H^+$ in Supersonic Jets. *Chem. Phys. Lett.* **1987**, *141*, 7−11.
(23) Storchi, L.; et al. The Auger Spectroscopy of Pyrimidine and Halogen-Substituted Pyrimidines. *J. Chem. Phys.* **2008**, *129*, 154309.
(24) Pokapanich, W.; et al. Ionic-Charge Dependence of the Intermolecular Coulombic Decay Time Scale for Aqueous Ions Probed by the Core-Hole Clock. *J. Am. Chem. Soc.* **2011**, *133*, 13430−13436.
(25) Hans, A.; et al. Core-Level Interatomic Coulombic Decay in van der Waals Clusters. *Phys. Rev. Research* **2020**, *2*, 12022.
(26) Slavíček, P.; Winter, B.; Cederbaum, L. S.; Kryzhevoi, N. V. Proton-Transfer Mediated Enhancement of Nonlocal Electronic Relaxation Processes in X-ray Irradiated Liquid Water. *J. Am. Chem. Soc.* **2014**, *136*, 18170−18176.
(27) Aziz, E. F.; Ottosson, N.; Faubel, M.; Hertel, I. V.; Winter, B. Interaction Between Liquid Water and Hydroxide Revealed by Core-Hole De-Excitation. *Nature* **2008**, *455*, 89−91.
(28) Kryzhevoi, N. V.; Cederbaum, L. S. Exploring Protonation and Deprotonation Effects with Auger Electron Spectroscopy. *J. Phys. Chem. Lett.* **2012**, *3*, 2733−2737.
(29) Jahnke, T. Interatomic and Intermolecular Coulombic Decay: The Coming of Age Story. *J. Phys. B: At., Mol. Opt. Phys.* **2015**, *48*, 082001.
(30) Thürmer, S.; et al. On the Nature and Origin of Dicationic, Charge-Separated Species Formed in Liquid Water on X-ray Irradiation. *Nat. Chem.* **2013**, *5*, 590−596.
(31) Ren, X.; et al. Experimental Evidence for Ultrafast Intermolecular Relaxation Processes in Hydrated Biomolecules. *Nat. Phys.* **2018**, *14*, 1062−1066.
(32) Jahnke, T.; et al. Interatomic and Intermolecular Coulombic Decay. *Chem. Rev.* **2020**, *120*, 11295−11369.
(33) Castrovilli, M. C.; et al. Photofragmentation of Halogenated Pyrimidine Molecules in the VUV Range. *J. Am. Soc. Mass Spectrom.* **2014**, *25*, 351−367.
(34) Cederbaum, L. S.; Zobeley, J.; Tarantelli, F. Giant Intermolecular Decay and Fragmentation of Clusters. *Phys. Rev. Lett.* **1997**, *79*, 4778−4781.
(35) Trinter, F.; et al. Resonant Auger Decay Driving Intermolecular Coulombic Decay in Molecular Dimers. *Nature* **2014**, *505*, 664−666.
(36) Gokhberg, K.; Kolorenč, P.; Kuleff, A. I.; Cederbaum, L. S. Site- and Energy-Selective Slow-Electron Production through Intermolecular Coulombic Decay. *Nature* **2014**, *505*, 661−663.
(37) Schwartz, C. P.; Fatehi, S.; Saykally, R. J.; Prendergast, D. Importance of Electronic Relaxation for Inter-Coulombic Decay in Aqueous Systems. *Phys. Rev. Lett.* **2010**, *105*, 198102.
(38) Mohamad, O.; et al. Carbon Ion Radiotherapy: A Review of Clinical Experiences and Preclinical Research, with an Emphasis on DNA Damage/Repair. *Cancers* **2017**, *9*, 66.
(39) Viefhaus, J.; et al. The Variable Polarization XUV Beamline P04 at PETRA III: Optics, Mechanics and their Performance. *Nucl. Instrum. Methods Phys. Res., Sect. A* **2013**, *710*, 151−154.
(40) Eland, J. H.; Feifel, R. Double Ionisation of ICN and BrCN Studied by a New Photoelectron-Photoion Coincidence Technique. *Chem. Phys.* **2006**, *327*, 85−90.

https://doi.org/10.1021/acs.jpclett.1c01879
J. Phys. Chem. Lett. 2021, 12, 7146−7150